E2-95-266



A.A.Bel'kov, A.V.Lanyov, S.Scherer*

# PROCESSES $\gamma\gamma \to \pi^0\pi^0$ AND $\eta \to \pi^0\gamma\gamma$ AT $O(p^6)$ IN THE NJL MODEL

Submitted to «Physics Letters B»

*Institut für Kernphysik, Johannes Gutenberg-Universität, D-55099 Mainz, Germany
Supported by Deutsche Forschungsgemeinschaft

1995

The theoretical interest in the reaction $\gamma\gamma \to \pi^0\pi^0$ dates back to the seventies when predictions for the electromagnetic polarizabilities of the charged as well as the neutral pion were obtained in the framework of current–algebra techniques [1] and chiral quantum field theory [2]. These polarizabilities are a signature of the underlying structure of particles, similar to the electromagnetic root–mean–square radius, and a large number of different predictions for these parameters has been obtained in various models (for an overview see, e.g., Refs. [3]). The possibility of investigating the $\gamma\gamma \to \pi^0\pi^0$ amplitude via the $e^+e^-$–annihilation process as well as the photoproduction in the Coulomb field of a nucleus was addressed in Refs. [4].

In the meantime, $\gamma\gamma \to \pi^0\pi^0$ cross section data from threshold up to the $\rho$-resonance region were provided by the Crystal Ball Collaboration [5]. On the theoretical side the framework of Chiral Perturbation Theory (ChPT) [6, 7] provides an ideal tool to systematically study low–energy amplitudes involving Goldstone bosons and their interactions with external fields, such as the electromagnetic field. In Refs. [8] the amplitude for $\gamma\gamma \to \pi^0\pi^0$ was calculated to $O(p^4)$ in ChPT, and the result was found to be given entirely in terms of one–loop diagrams involving vertices of $O(p^2)$. In other words, there are no tree–level diagrams at $O(p^2)$ and $O(p^4)$ and thus the one–loop diagrams are finite. However, the one–loop calculation in ChPT disagrees with the data even near threshold. The inclusion of a Born contribution at $O(p^6)$, obtained either from quark loops or from vector–meson dominance, results in too small a contribution to yield agreement with experiment [9]. On the other hand, the application of dispersive methods leads to a considerable improvement since they take account of important unitarity corrections corresponding to rescattering effects of higher order [10]. A full two–loop calculation at $O(p^6)$ within $SU(2)\times SU(2)$ ChPT was carried out in Ref. [11]. The $O(p^6)$ counterterm contributions were estimated with resonance saturation and the total result was found to be in good agreement up to an invariant mass $\sqrt{s}$ of 700 MeV. Finally, $\gamma\gamma \to \pi^0\pi^0$ was also considered in the context of Generalized ChPT up to one–loop order corresponding to $O(p^5)$ in this counting scheme [12].

In the framework of chiral $SU(3) \times SU(3)$ symmetry the decay process $\eta \to \pi^0\gamma\gamma$ is closely related to $\gamma\gamma \to \pi^0\pi^0$. At $O(p^4)$ in ChPT the prediction for the decay width [13] was found to be two orders of magnitude smaller than the measured value [14]. The pion loops are small due to approximate $G$–parity invariance whereas the kaon loops are suppressed by the large kaon mass in the propagator. A considerable enhancement was obtained with resonance saturation for some counterterms of higher orders in the momentum expansion. In Ref. [13] symmetry–breaking terms

proportional to the quark masses were not considered at $O(p^6)$. Such counterterms were, however, included in Refs. [15, 16]. In Ref. [15] they were estimated in the framework of an extended NJL model [17] whereas in Ref. [16] the experimental decay width was used to fit one of the corresponding coefficients. Finally, a complementary approach was used in Ref. [18] where the $\eta \to \pi^0\gamma\gamma$ decay was calculated in a phenomenological quark model using the quark–box diagram. A good agreement with the experimental value for the decay width was obtained with a constituent quark mass of 300 MeV.

It is the purpose of this work to present the results of a consistent calculation of the processes $\gamma\gamma \to \pi^0\pi^0$ and $\eta \to \pi^0\gamma\gamma$ at $O(p^6)$ in the momentum expansion. According to Weinberg's power counting scheme [6] the calculation involves tree–level, one– and two–loop diagrams. The effective action up to $O(p^6)$ in terms of collective meson degrees of freedom is obtained by bosonization [19] of the NJL model [20]. This effective action, in addition to the pseudoscalar mesons, still contains scalar, vector and axial vector degrees of freedom. In order to determine the structure coefficients of the effective chiral lagrangian at $O(p^4)$ [7] and $O(p^6)$ [21] one has to integrate out the meson resonances. The method of superpropagator regularization [22] was used in order to fix the UV divergences which for the first time show up at $O(p^6)$.

We start from the generating functional

$$\mathcal{Z} = \int \mathcal{D}\Phi\, \mathcal{D}\Phi^\dagger\, \mathcal{D}V\, \mathcal{D}A\, \exp[i\mathcal{S}(\Phi, \Phi^\dagger, V, A)]\,, \tag{1}$$

corresponding to the following action for scalar ($S$), pseudoscalar ($P$), vector ($V_\mu$) and axial vector ($A_\mu$) collective meson fields,

$$\begin{aligned}\mathcal{S}(\Phi, \Phi^\dagger, V, A) \;=\; \int d^4x \Big\{ &-\frac{1}{4G_1}\mathrm{tr}(\Phi^\dagger\Phi) - \frac{1}{4G_2}\mathrm{tr}(V_\mu V^\mu + A_\mu A^\mu) \\ &+ \log(\det(i\widehat{\mathbf{D}}))\Big\}. \end{aligned} \tag{2}$$

This action is obtained by first bosonizing the effective action of the NJL model and then integrating over the quark degrees of freedom. In Eq. (2) $G_1$ and $G_2$ are parameters which are fitted to empirical input (see Eqs. (11) and (13) below for details), $\Phi = S + iP$, and $\widehat{\mathbf{D}}$ refers to the Dirac operator

$$i\widehat{\mathbf{D}} = \not{\partial} + \not{A}_R) - (\Phi + m_0)]P_R + [i(\not{\partial} + \not{A}_L) - (\Phi + m_0)^\dagger]P_L, \tag{3}$$

where $m_0$ is the current quark mass matrix, $P_{R/L} = \frac{1}{2}(1 \pm \gamma_5)$ are chiral projectors and $A_\mu^{R/L} = V_\mu \pm A_\mu$. The electromagnetic interaction can be included by the replacement

$V_\mu \to V_\mu + ie\mathcal{A}_\mu Q$, where $Q$ is the quark charge matrix, $Q = \mathrm{diag}(2/3, -1/3, -1/3)$. We express $\Phi$ using a nonlinear realization of chiral symmetry,

$$\Phi = \Omega \Sigma \Omega,$$

where

$$\Omega(x) = \exp\left(\frac{i}{\sqrt{2}F_0}\varphi(x)\right),$$

$$\varphi = \begin{pmatrix} \frac{1}{\sqrt{2}}\pi^0 + \frac{1}{\sqrt{6}}\eta_8 + \frac{1}{\sqrt{3}}\eta_0 & \pi^+ & K^+ \\ \pi^- & -\frac{1}{\sqrt{2}}\pi^0 + \frac{1}{\sqrt{6}}\eta_8 + \frac{1}{\sqrt{3}}\eta_0 & K^0 \\ K^- & \bar{K}^0 & -\sqrt{\frac{2}{3}}\eta_8 + \frac{1}{\sqrt{3}}\eta_0 \end{pmatrix} \tag{4}$$

represents the pseudoscalar degrees of freedom. $F_0$ is the bare $\pi$ decay constant. The $3 \times 3$ matrix $\Sigma(x)$ contains the scalar fields and is expanded around its vacuum expectation value $\mu$,

$$\Sigma(x) = \mu + \sigma(x). \tag{5}$$

The constituent quark mass $\mu$ is the solution of the gap equation.

For the processes under consideration, up to and including $O(p^6)$, only the even intrinsic-parity sector of the chiral lagrangian is required [13]. This sector is obtained from the modulus of the logarithm of the quark determinant and can be calculated using the heat-kernel technique with proper-time regularization [23, 24]. This method has been used in Ref. [25] to obtain a prediction for the structure coefficients of the general effective lagrangian of $O(p^4)$ and $O(p^6)$, respectively [7, 21]. The result of Ref. [25] explicitly contains, apart from the pseudoscalar Goldstone bosons, scalar, vector and axial-vector resonances as *dynamical* degrees of freedom. However, in order to avoid double counting when calculating processes involving Goldstone bosons and photons, one has to integrate out (reduce) these resonances in the generating functional of Eq. (1) and thus one effectively takes resonance exchange contributions into account. As a consequence of this procedure the structure coefficients of pseudoscalar low-energy interactions will be strongly modified [17, 26, 27].

In order to perform the integration over the scalar, vector and axial-vector fields in Eq. (1) we made use of the fact that the modulus of the quark determinant in Eq. (2) is invariant under local chiral transformations of the fields [27, 28]. This allows us, with a specific choice for the chiral transformation (unitary gauge), to eliminate the pseudoscalar fields from the Dirac operator, Eq. (3). At the same time, introducing $\Phi' = \Phi - m_0$ and renaming $\Phi' \to \Phi$ generates the mass term for the pseudoscalars from the Gaussian part of Eq. (2). Furthermore, interactions

between the pseudoscalar degrees of freedom and the transformed vector and axial-vector fields are generated in the Gaussian part. The masses of the scalar, vector and axial-vector mesons are sufficiently large in comparison with the Goldstone boson masses, and thus it is possible to integrate out the meson resonances using their respective equations of motion in the static limit. These equations result from a variation of the effective action of Eq. (2) by neglecting terms of $O(p^4)$ and higher in the logarithm of the quark determinant. The remaining part of the action then is quadratic in the resonances, in particular, there are no terms containing field strength tensors.

The invariant amplitude $\mathcal{M} = i\epsilon_1^\mu \epsilon_2^\nu T_{\mu\nu}$ of the process $\gamma(q_1)\gamma(q_2) \to a(p_1)b(p_2)$ can be expressed in terms of two functions $A$ and $B$ as

$$\begin{aligned} T_{\mu\nu}^{\gamma\gamma\to ab} &= A(s,\nu)\left(\frac{s}{2}g_{\mu\nu} - q_{2\mu}q_{1\nu}\right) \\ &\quad + B(s,\nu)\Big[2s\Delta_\mu\Delta_\nu - \left(\nu^2 - (m_b^2 - m_a^2)^2\right)g_{\mu\nu} \\ &\quad + 2\Big((\nu + m_b^2 - m_a^2)q_{2\mu}\Delta_\nu - (\nu + m_a^2 - m_b^2)\Delta_\mu q_{1\nu}\Big)\Big], \end{aligned} \tag{6}$$

where $s = (q_1 + q_2)^2$, $\nu = 2p_1\cdot(q_2 - q_1)$, and $\Delta_\mu = (p_1 - p_2)_\mu$. The amplitude for the process $a(p_1) \to b(p_2)\gamma(q_1)\gamma(q_2)$ can be obtained from Eq. (6) using crossing symmetry, namely, by performing the replacement $q_i \to -q_i$ and $p_1 \to -p_1$. However, for the decay channel $\eta(k) \to \pi^0(p)\gamma(q_1)\gamma(q_2)$, it turns out to be more convenient to use the parameterization

$$\begin{aligned} T_{\mu\nu}^{(\eta\to\pi^0\gamma\gamma)} &= \mathcal{A}(x_1,x_2)[g_{\mu\nu}(q_1\cdot q_2) - q_{1\nu}q_{2\mu}] \\ &\quad + \mathcal{B}(x_1,x_2)\left[m_\eta^2 x_1 x_2 g_{\mu\nu} + \frac{(q_1\cdot q_2)}{m_\eta^2}k_\mu k_\nu - x_1 q_{2\mu}k_\nu - x_2 k_\mu q_{1\nu}\right], \end{aligned} \tag{7}$$

where $x_i = (k\cdot q_i)/m_\eta^2$.

The prediction for the amplitudes of Eqs. (6) and (7) will involve the structure coefficients $L_i$ of the Gasser–Leutwyler lagrangian in one-loop diagrams at $O(p^6)$ as well as new coefficients $d_i$ from Born diagrams at $O(p^6)$. It is straightforward to obtain the effective lagrangian at $O(p^6)$ contributing to the processes under consideration from the most general representation of Ref. [21]. [1]

$$\begin{aligned} \mathcal{L}_6 &= \frac{8}{F_0^2}\Big[d_1\mathcal{F}_{\mu\alpha}\mathcal{F}^{\mu\beta}\mathrm{tr}\left(\partial^\alpha U_0\partial_\beta U_0^\dagger Q^2\right) + d_2\mathcal{F}_{\mu\nu}\mathcal{F}^{\mu\nu}\mathrm{tr}\left(\partial_\alpha U_0\partial^\alpha U_0^\dagger Q^2\right) \\ &\quad + d_3\mathcal{F}_{\mu\nu}\mathcal{F}^{\mu\nu}\mathrm{tr}\left(\chi(U_0 + U_0^\dagger)Q^2\right) + d_4\mathcal{F}_{\mu\nu}\mathcal{F}^{\mu\nu}\mathrm{tr}(Q^2)\mathrm{tr}\left(\chi(U_0 + U_0^\dagger)\right) \\ &\quad + d_5\mathcal{F}_{\mu\alpha}\mathcal{F}^{\mu\beta}\mathrm{tr}\left(Q^2\right)\mathrm{tr}\left(\partial^\alpha U_0\partial_\beta U_0^\dagger\right) + d_6\mathcal{F}_{\mu\nu}\mathcal{F}^{\mu\nu}\mathrm{tr}\left(Q^2\right)\mathrm{tr}\left(\partial_\alpha U_0\partial^\alpha U_0^\dagger\right) \end{aligned}$$

[1] Note that there are different conventions for the definition of the coefficients $d_i$.

$$+d_7\mathcal{F}_{\mu\alpha}\mathcal{F}^{\mu\beta}\mathrm{tr}\left(\partial^\alpha U_0 U_0^\dagger Q\right)\mathrm{tr}\left(\partial_\beta U_0 U_0^\dagger Q\right)$$
$$+d_8\mathcal{F}_{\mu\nu}\mathcal{F}^{\mu\nu}\mathrm{tr}\left(\partial_\alpha U_0 U_0^\dagger Q\right)\mathrm{tr}\left(\partial^\alpha U_0 U_0^\dagger Q\right)\Big]\,. \tag{8}$$

In Eq. (8), $\mathcal{F}_{\mu\nu} = \partial_\mu\mathcal{A}_\nu - \partial_\nu\mathcal{A}_\mu$ is the ordinary electromagnetic field strength tensor,

$$U_0 = \exp(i\frac{\sqrt{2}\varphi_0}{F_0}),$$

$$\varphi_0 = \mathrm{diag}\left(\frac{\pi^0}{\sqrt{2}} + \frac{\eta_8}{\sqrt{6}} + \frac{1}{\sqrt{3}}\eta_0, -\frac{\pi^0}{\sqrt{2}} + \frac{\eta_8}{\sqrt{6}} + \frac{1}{\sqrt{3}}\eta_0, -\sqrt{\frac{2}{3}}\eta_8 + \frac{1}{\sqrt{3}}\eta_0\right),$$

and $\chi \equiv \mathrm{diag}(\chi_u^2, \chi_d^2, \chi_s^2) = -2m_0 <\bar{q}q> F_0^{-2}$ is the mass matrix, where $<\bar{q}q>$ is the quark condensate. Previous calculations considered the counterterms of Eq. (8) with various degrees of approximation. In Ref. [13] only single–trace terms in the chiral limit were taken into account. In Refs. [11, 15] the chiral symmetry breaking term proportional to $d_3$ was included and Ref. [16] also took $d_4$ into account. The double–trace terms proportional to $d_4 - d_8$ typically do not appear in effective lagrangians derived from the bosonization of NJL type quark models.

In the NJL model only the structure constants $d_1$, $d_2$, $d_3$ contribute to the Born amplitudes of the processes $\gamma\gamma \to \pi^0\pi^0$ and $\eta \to \pi^0\gamma\gamma$ at $O(p^6)$, respectively,

$$\begin{aligned} A^{B(p^6)} &= \frac{64e^2}{9F_0^4}\Big[\frac{5}{16}d_1 s + \frac{5}{2}d_2(s - 2m_\pi^2) + d_3(4\chi_u^2 + \chi_d^2)\Big]\,, \\ B^{B(p^6)} &= -\frac{10e^2}{9F_0^4}d_1\,. \end{aligned} \tag{9}$$

and

$$\begin{aligned} \mathcal{A}^{B(p^6)} &= \frac{8e^2}{3\sqrt{3}F_0^4}C_\theta\Big\{2(d_1+4d_2)m_\eta^2(x_1+x_2) - \frac{8}{3}\Big[3d_2m_\eta^2 + d_3(-4\chi_u^2+\chi_d^2)\Big] \\ &\quad + \frac{\chi_u^2-\chi_d^2}{6(m_\eta^2-m_\pi^2)}\Big[(d_1+4d_2)m_\eta^2(x_1+x_2) - 4d_2m_\eta^2 + 4d_3(4\chi_u^2+\chi_d^2)\Big] \\ &\quad - \frac{1}{3}(\chi_u^2-\chi_d^2)\Theta_1\Big[(d_1+4d_2)m_\eta^2(x_1+x_2) \\ &\qquad - \frac{4}{3}\Big(d_2m_\eta^2 - d_3(4\chi_u^2+\chi_d^2+4\chi_s^2)\Big)\Big]\Big\}\,, \\ \mathcal{B}^{B(p^6)} &= -\frac{16e^2}{3\sqrt{3}F_0^4}C_\theta\Big[2 + \frac{5}{3}\frac{\chi_u^2-\chi_d^2}{m_\eta^2-m_\pi^2} + \frac{1}{3}(\chi_u^2-\chi_d^2)\Theta_1\Big]m_\eta^2 d_1\,. \end{aligned} \tag{10}$$

In Eqs. (10) $C_\theta = \cos\theta - \sqrt{2}\sin\theta$, where $\theta = -19^\circ$ is the $\eta-\eta'$ mixing angle,

$$\eta_8 = \eta\cos\theta + \eta'\sin\theta\,, \quad \eta_0 = -\eta\sin\theta + \eta'\cos\theta\,,$$

and furthermore we have introduced

$$\Theta_1 = \frac{(\cos\theta - \sqrt{2}\sin\theta)^2}{m_\eta^2 - m_\pi^2} + \frac{(\sin\theta + \sqrt{2}\cos\theta)^2}{m_{\eta'}^2 - m_\pi^2}.$$

Note that the $\eta$ decay amplitudes of Eqs. (10) also include contributions of the pole diagrams with $\pi^0 - \eta$ and $\pi^0 - \eta'$ transitions.

We now turn to the determination of the structure coefficients within the framework of the NJL model. It is a well-known fact that the elimination of the resonance degrees of freedom gives rise to a substantial modification of the structure constants. At $O(p^2)$ such a reduction leads to a redefinition of the decay constant $F_0$ and the mass matrix $\chi$. To be specific, the identification of the decay constant before and after reduction is given by

$$F_0^2 = \frac{N_c \mu^2 y}{4\pi^2} \quad \longrightarrow \quad F_0^2 = Z_A^2 \frac{N_c \mu^2 y}{4\pi^2}, \tag{11}$$

respectively, and similarly [2] for $\chi$

$$\chi = -2m_0\mu\left(1 - \frac{\Lambda^2}{y\mu^2} e^{-\mu^2/\Lambda^2}\right) \quad \longrightarrow \quad \chi = \frac{m_0\mu}{G_1 F_0^2}, \tag{12}$$

where $y = \Gamma(0, \mu^2/\Lambda^2)$, $\mu$ is the average constituent quark mass, $\Lambda$ is the intrinsic cutoff parameter, and

$$Z_A^{-2} = 1 + \left(\frac{g_V^0}{m_V^0}\right)^2 \frac{N_c \mu^2 y}{4\pi^2}, \quad \left(\frac{m_V^0}{g_V^0}\right)^2 = \frac{1}{4G_2}. \tag{13}$$

The incomplete gamma function is defined as $\Gamma(n, x) = \int_x^\infty dt\, e^{-t} t^{n-1}$. In Eq. (13) we have introduced

$$g_V^0 = \left[\frac{N_c}{48\pi^2}(2y - 1)\right]^{-1/2}, \quad (m_V^0)^2 = m_\rho^2(1 + \tilde{\gamma}), \quad \tilde{\gamma} = \frac{N_c (g_V^0)^2}{48\pi^2}.$$

The parameter $Z_A^2$ of Eq. (13) corresponds to the $\pi - A_1$ mixing factor and has the phenomenological value

$$Z_A^2 = \frac{m_\rho^2}{m_{A_1}^2} \frac{1 + \tilde{\gamma}}{1 - \tilde{\gamma}} \approx 0.62,$$

where we used the following empirical input, $m_\rho = 770$ MeV, $m_{A_1} = 1260$ MeV, and $g_V = g_{\rho\pi\pi} = 6.3$. On the other hand, with the special choice $Z_A^2 = 1/2$, Eqs. (13) and (11) reproduce the well-known Kawarabayashi-Suzuki relation, $m_\rho^2 = 2g_V^2 F_0^2$.

[2] Using the gap equation it can be shown that both expressions for $\chi$ in Eqs. (12) are equivalent for $\mu^2/\Lambda^2 \ll 1$.

A full calculation of the $\pi$ and $K$ decay constants at $O(p^4)$ allows to fix the parameters $y$ and $x = -\mu F_0^2/(2<\bar{q}q>)$ for given values of $Z_A^2$ and $\mu$, by identifying the decay constants with their empirical values. In the following we will use $Z_A^2 = 0.62$ and $\mu = 265$ MeV, from which we obtain $y = 2.4$ and $x = 0.10$. These values correspond to $F_0 = 90$ MeV and $<\bar{q}q>^{1/3} = -220$ MeV.

At $O(p^4)$ the reduction of the resonances [27] leads to the following modification of the structure coefficients of the lagrangian introduced by Gasser and Leutwyler [7] ($L_i = \frac{N_c}{16\pi^2} l_i$),

$$
\begin{aligned}
l_1 &= \frac{1}{24}, & l_1^{red} &= \frac{1}{24}\Big[Z_A^8 + 2(Z_A^4-1)\Big(\frac{1}{4}y(Z_A^4-1) - Z_A^4\Big)\Big] = 1.08\, l_1;\\
l_2 &= 2l_1, & l_2^{red} &= 2l_1^{red};\\
l_3 &= -\frac{1}{6}, & l_3^{red} &= -\frac{1}{6}\Big[Z_A^8 + 3(Z_A^4-1)\Big(\frac{1}{4}y(Z_A^4-1) - Z_A^4\Big)\Big] = 1.54\, l_3;\\
l_4 &= 0, & l_4^{red} &= 0;\\
l_5 &= x(y-1), & l_5^{red} &= (y-1)\frac{1}{4}Z_A^6 = 0.60\, l_5;\\
l_6 &= 0, & l_6^{red} &= 0;\\
l_7 &= -\frac{1}{6}\Big(xy - \frac{1}{12}\Big), & l_7^{red} &= 0;\\
l_8 &= \Big(\frac{1}{2} - x\Big)xy - \frac{1}{24}, & l_8^{red} &= \frac{y}{16}Z_A^4 = 1.07\, l_8;\\
l_9 &= \frac{1}{3}, & l_9^{red} &= \frac{1}{3}\Big(Z_A^4 - \frac{1}{2}y(Z_A^4-1)\Big) = 1.12\, l_9;\\
l_{10} &= -\frac{1}{6}, & l_{10}^{red} &= -\frac{1}{6}\Big(Z_A^4 - y(Z_A^4-1)\Big) = 1.86\, l_{10}.
\end{aligned}
\tag{14}
$$

In order to obtain the expressions for the reduced coefficients of Eq. (14), the static equations of motion of the scalar, vector and axial vector resonances have been applied. In such an approach scalar resonances can only modify $l_5$ and $l_8$. Note that the above results are in agreement with those obtained in Ref. [17] except for $l_3^{red}$ and $l_8^{red}$ (see Sect. 5.5 of Ref. [17]). The disagreement originates in a different procedure of integrating out the scalar resonances. We will come back to this point below when discussing higher order corrections to the static equations of motion.

We will now discuss those structure constants $d_i$ at $O(p^6)$ which do not vanish in the NJL model. Before reduction we obtain

$$
\begin{aligned}
d_1 &= -\frac{N_c}{16\pi^2}\frac{F_0^2}{\mu^2}\frac{1}{24} = -9.13\times 10^{-5}, \quad d_2 = \frac{N_c}{16\pi^2}\frac{F_0^2}{\mu^2}\frac{1}{48} = 4.57\times 10^{-5},\\
d_3 &= \frac{N_c}{16\pi^2}\frac{F_0^2}{\mu^2}\frac{1}{12}x = 1.83\times 10^{-5}.
\end{aligned}
\tag{15}
$$

The first two constants coincide with the results of Ref. [9]. The reduction of meson

resonances in the framework of applying the static equations of motion generates the following modifications

$$d_1^{red} = -\frac{N_c}{16\pi^2}\frac{F_0^2}{\mu^2}\frac{1}{24}Z_A^4 = -3.51\times 10^{-5}\,, \quad d_2^{red} = \frac{N_c}{16\pi^2}\frac{F_0^2}{\mu^2}\frac{1}{48}Z_A^4 = 1.76\times 10^{-5}\,,$$
$$d_3^{red} = \frac{N_c}{16\pi^2}\frac{F_0^2}{\mu^2}\frac{1}{96}Z_A^2 = 1.42\times 10^{-5}\,. \tag{16}$$

In this context we note that the modification of the first two structure coefficients results from the application of the equation of motion to vector and axial-vector resonances. This change amounts to a multiplication of the original coefficients $d_1$ and $d_2$ of Eq. (15) by a factor $Z_A^4$. The situation for $d_3$ is qualitatively different. In this case the application of the equation of motion to the *scalar* resonances modifies this coefficient. Let us compare our results for $d_i^{red}$ with those of Ref. [15]. We agree for the coefficients $d_1^{red}$ and $d_3^{red}$ but differ with respect to $d_2^{red}$. In order to understand this discrepancy we note that two different techniques were used to eliminate the resonances. In the treatment of scalar resonances the method of Ref. [15] involves operators with derivatives which are beyond the scope of our treatment using the static equation of motion. A comparison with Eqs. (23), (32) and (38) of Ref. [15] shows that such operators are the origin for the difference in $d_2^{red}$. However, there is another interesting observation. Even though our final expression for $d_3^{red}$ is the same as Eq. (40) of Ref. [15] our result originates entirely from the reduction of scalar resonances whereas in Ref. [15] it is the sum of a scalar resonance contribution (see Eq. (39)) and a quark loop contribution (see Eq. (23)) for which we have no analogue.

Finally, we have also investigated in our approach those results of Ref. [15] which correspond to the inclusion of operators containing derivatives when integrating out the scalar resonance. To this end, after a unitary gauge transformation of the modulus of the quark determinant, one has to keep also higher order terms in the effective action of Eq. (2) which are linear in the scalar field $\sigma(x)$ and which contain the coupling to vector, axial vector fields and field strength tensors. Such higher-order terms lead to a modification of the static equation of motion for the scalar resonances and thus give an *additional* contribution to the structure coefficients $l_3^{red}$ and $d_2^{red}$.

$$l_3^{red(h.o.)} = \frac{1}{4}\frac{(y-1)^2}{y}Z_A^8 = -0.18 l_3\,, \tag{17}$$

$$d_2^{red(h.o.)} = \frac{N_c}{16\pi^2}\frac{F_0^2}{\mu^2}\frac{1}{48}\frac{y-1}{y}Z_A^4 = 1.02\times 10^{-5}\,, \tag{18}$$

Table 1. Modification of the coefficients $a_1$, $a_2$ and $b$ of Eq. (19) due to the reduction of meson resonances. $\mathcal{N} = N_c(4\pi F_0/\mu)^2 = 54.6$, $Z_A^2 = 0.62$

| Coeff. | Without reduction | Reduction of resonances | | | Sum |
|---|---|---|---|---|---|
| | | $V_\mu$– and $A_\mu$–fields | $\sigma$–field | | |
| | | in static approx. | Static approx. | Higher–order correct. | |
| $a_1$ | $\frac{20}{27}(13x-1)\mathcal{N} = 12.1$ | $-\frac{20}{27}Z_A^4\mathcal{N} = -15.6$ | $\frac{10}{27}Z_A^2\mathcal{N} = 12.5$ | $-\frac{20}{27}Z_A^2\left(1-\frac{1}{y}\right)\mathcal{N} = -9.0$ | -12.1 |
| $a_2$ | $\frac{5}{18}\mathcal{N} = 15.2$ | $\frac{5}{18}Z_A^4\mathcal{N} = 5.8$ | 0 | $\frac{10}{27}Z_A^4\left(1-\frac{1}{y}\right)\mathcal{N} = 4.5$ | 10.3 |
| $b$ | $\frac{5}{108}\mathcal{N} = 2.53$ | $\frac{5}{108}Z_A^4\mathcal{N} = 0.97$ | 0 | 0 | 0.97 |

which agree with Eq. (155) of Ref. [17] and Eq. (38) of Ref. [15], respectively. The total result for the coefficients $l_3^{red}$ and $d_2^{red}$ after reduction of the vector, axial–vector and scalar degrees of freedom then are the sum of the contributions of Eqs. (14) and (17) and (16) and (18), respectively. It is worth noting that the considered higher-order terms also modify the static equation of motion of axial–vector resonances. However, this modification does not lead to any new contributions for either the structure coefficients $L_i$ or $d_i$.

For the purpose of comparing our numerical results for $\gamma\gamma \to \pi^0\pi^0$ with those of Refs. [11, 15], it is convenient to introduce the following parameterization [11] of the Born contribution at $O(p^6)$ for the amplitudes $A$ and $B$ of Eq. (6),

$$A_6 = \frac{a_1 m_\pi^2 + a_2 s}{(16\pi^2 F_0^2)^2}, \quad B_6 = \frac{b}{(16\pi^2 F_0^2)^2}. \tag{19}$$

The coefficients $a_1$, $a_2$ and $b$ are related to $d_1$, $d_2$ and $d_3$ by

$$a_1 = (4\pi)^4 \frac{10}{9} 32(d_3 - d_2), \quad a_2 = (4\pi)^4 \frac{10}{9} 2(d_1 + 8d_2), \quad b = -(4\pi)^4 \frac{10}{9} d_1 .$$

Our results for $a_i$ and $b$ are summarized in Table 1. Clearly, the reduction of the resonances leads to a large modification of the coefficients. However, one has to keep in mind that the effective action after the reduction describes the interaction of only pseudoscalars and photons. Thus the modified coefficients should not be treated as *additional* corrections to the nonreduced coefficients of Eq. (15). A summation of quark–loop contributions and resonance–exchange contributions to the structure coefficients as in Table 1 of Ref. [15], in our opinion, leads to double counting.

Before comparing our values of the $O(p^6)$ structure coefficients with those of Ref. [11] we provide a prescription for relating results in different renormalization schemes. In our approach UV divergences, resulting from meson loops at $O(p^6)$, were separated using the superpropagator regularization method [22] which is particularly well-suited for the treatment of loops in nonlinear chiral theories. The result is equivalent

to the dimensional regularization technique used in Ref. [11], the difference being that the scale parameter $\mu$ is no longer arbitrary but fixed by the inherent scale of the chiral theory, namely, $\tilde{\mu} = 4\pi F_0$. In order to compare the two methods the UV divergences have to be replaced by a finite term using the substitution

$$(C - 1/\varepsilon) \quad \longrightarrow \quad C_{SP} = 2C + 1 + \frac{1}{2}\left[\frac{d}{dz}\left(\log\Gamma^{-2}(2z+2)\right)\right]_{z=0} + \beta\pi = -1 + 4C + \beta\pi\,,$$

where $C = 0.577$ is Euler's constant, $\varepsilon = (4 - D)/2$, and $\beta$ is an arbitrary constant resulting from the Sommerfeld–Watson integral representation of the superpropagator. The splitting of the decay constants $F_\pi$ and $F_K$ is used at $O(p^4)$ to fix $C_{SP} \approx 3.0$. For our numerical comparison with the two–loop calculation of Ref. [11] we made use of the parameters $L_i$ and $d_i$ corresponding to Tables 1 and 2 of Ref. [11]. In particular, from the numerical values of the parameters $a_1$, $a_2$ and $b$ of Table 2 of Ref. [11]

$$a_1^{BGS} = -39.0\,, \quad a_2^{BGS} = 12.5\,, \quad b^{BGS} = 3.0$$

one obtains

$$d_1^{BGS} = -10.8 \times 10^{-5}\,, \quad d_2^{BGS} = 4.29 \times 10^{-5}\,, \quad d_3^{BGS} = -0.10 \times 10^{-5}\,. \qquad (20)$$

Our predictions at $O(p^4)$ and $O(p^6)$ for the $\gamma\gamma \to \pi^0\pi^0$ cross section near threshold are shown in Fig. 1. The calculation at $O(p^6)$ contains Born, one–loop and two loop diagrams. In our two–loop calculation only diagrams which are factorizable and which can be calculated analytically were taken into account. Two–loop box diagrams and acnode graphs cannot be calculated analytically but the numerical estimates of Ref. [11] indicate that their contributions are small. As was already discussed in Ref. [15], the predictions of the NJL model for the coefficients $d_1^{red}$ and $d_2^{red}$ are about a factor one half smaller in comparison with the vector–meson dominance model (VMD) (see, Refs. [9, 15]). The coefficients $d_1$ and $d_2$ in the VMD model can be obtained from Eq. (16) by the replacement

$$Z_A^4 \quad \longrightarrow \quad \tilde{Z}_A^4 = \frac{6}{N_c}\left(\frac{16\pi h_V \mu}{m_V}\right)^2 = 0.82, \qquad (21)$$

with $m_V = m_\rho$, and where the coupling constant $h_V = 3.7 \times 10^{-2}$ is extracted from the decays $V \to \pi\gamma$. This has to be compared with the prediction of the NJL model, $h_V^{NJL} = 2.5 \times 10^{-2}$ for $Z_A^2 = 0.62$. We have taken account of this uncertainty by showing the results for both $Z_A^2 = 0.62$ and $\tilde{Z}_A^2 = 0.91$. The results of our calculations with the parameters of Ref. [11] are also shown in Fig. 1. Numerically they are in

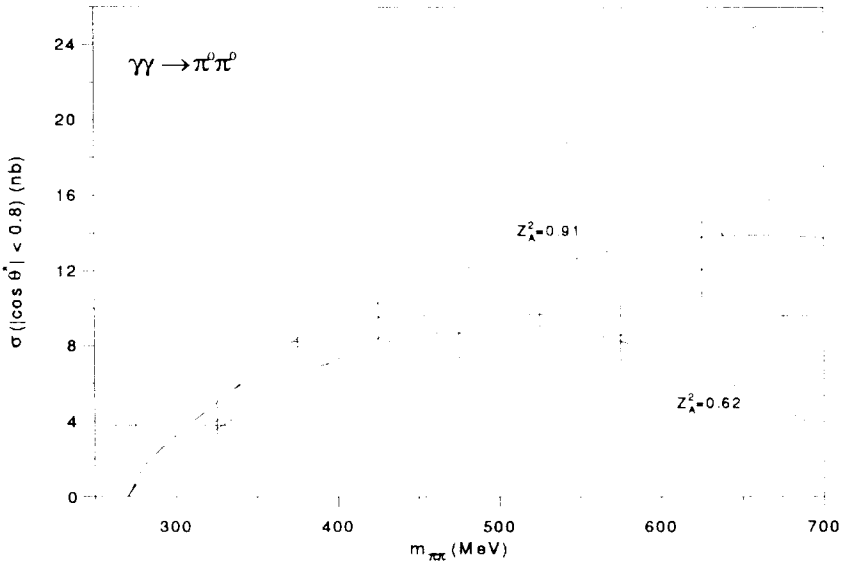


**Fig. 1.** Cross section for $\gamma\gamma \rightarrow \pi^0\pi^0$ as a function of the invariant mass $W = m_{\pi^0\pi^0}$ for $W < 0.7$ GeV and $|\cos\theta^*| < 0.8$ where $\theta^*$ is the angle between the beam axis and one of the $\pi^0$ in the $\gamma\gamma$ center of mass system (c.m.s). The data are from the Crystal Ball experiment [5]. The dotted line represents the one loop calculation at $O(p^4)$. The dashed line corresponds to the calculation at $O(p^6)$ without reduction of the resonance degrees of freedom. The dash-dotted lines corresponding to two different values of the parameter $Z_A^2$ are a measure for the uncertainty in the reduction of the meson resonances. This uncertainty is due to the difference between the NJL prediction and the empirical value for the coupling constant $h_V$. The solid line corresponds to the values of the coefficients $L_i$ and $d_i$ used in Ref. [11].

Table 2. Contribution of various diagrams to the $\eta \to \pi^0\gamma\gamma$ decay width.
$\Gamma^{exp}_{\eta\to\pi^0\gamma\gamma} = (0.84 \pm 0.18)$ eV

| Amplitudes | | Without reduction (eV) | With reduction (eV) | |
|---|---|---|---|---|
| | | | $Z_A^2 = 0.62$ | $Z_A^2 = 0.91$ |
| 1-loop $O(p^4)$ | $\pi\pi$-loops | $1.3 \cdot 10^{-3}$ | $1.3 \cdot 10^{-3}$ | $1.3 \cdot 10^{-3}$ |
| | $K\overline{K}$-loops | $6.2 \cdot 10^{-3}$ | $6.2 \cdot 10^{-3}$ | $6.2 \cdot 10^{-3}$ |
| Born $O(p^6)$ | | 0.22 | 0.11 | 0.45 |
| 1-loop $O(p^6)$ | $\pi\pi$-loops | $1.9 \cdot 10^{-4}$ | $6.9 \cdot 10^{-5}$ | $8.6 \cdot 10^{-4}$ |
| | $K\overline{K}$-loops | $4.1 \cdot 10^{-2}$ | $1.9 \cdot 10^{-3}$ | $2.7 \cdot 10^{-2}$ |
| 2-loop $O(p^6)$ | $\pi\pi$-loops | $3.2 \cdot 10^{-4}$ | $3.2 \cdot 10^{-4}$ | $3.2 \cdot 10^{-4}$ |
| | $\pi K$-loops | $3.1 \cdot 10^{-3}$ | $3.1 \cdot 10^{-3}$ | $3.1 \cdot 10^{-3}$ |
| | $K\overline{K}$-loops | $1.4 \cdot 10^{-5}$ | $1.4 \cdot 10^{-5}$ | $1.4 \cdot 10^{-5}$ |
| Total | | 0.14 | 0.11 | 0.35 |

a good agreement with Ref. [11]; even for $m_{\pi\pi}$ as large as 700 MeV the difference is only about 7%.

For the decay width of $\eta \to \pi^0\gamma\gamma$ we obtain after the reduction 0.11 eV and 0.35 eV corresponding to $Z_A^2 = 0.62$ and $Z_A^2 = 0.91$, respectively. On the other hand, using the parameters of Eq. (20) one finds 0.18 eV. These results have to be compared with the experimental value $(0.84 \pm 0.18)$ eV [14]. The contributions of different diagrams to the decay width are shown in Table 2. These results clearly show the dominance of the Born contribution. It is a well-known fact that calculations of the decay width at $O(p^6)$ tend to come out too small in comparison with the experimental value [13, 15, 16]. This failure indicates that either higher-order terms are required or higher order resonances have to be included or both.

Finally, we have also tried to fit the coefficients $d_1$, $d_2$ and $d_3$. However, due to a strong correlation between the coefficients $d_1$ and $d_3$ it was impossible to find a stable minimum from a fit to the $\gamma\gamma \to \pi^0\pi^0$ cross section and the $\eta \to \pi^0\gamma\gamma$ decay width. The strong correlation is related to the fact that the $m_{\pi\pi}$ dependence of the

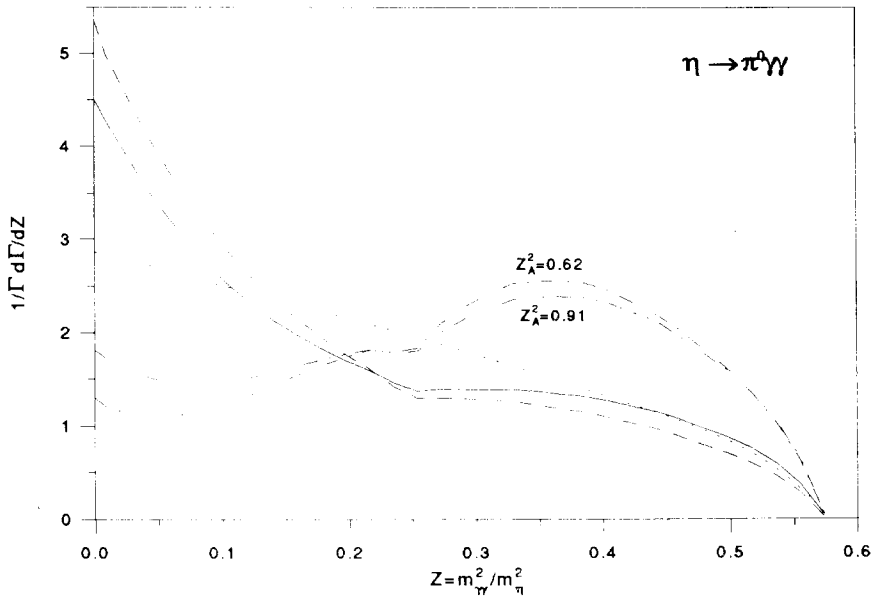


**Fig. 2.** Normalized differential decay probability for $\eta \to \pi^0\gamma\gamma$ as a function of $Z = m_{\gamma\gamma}^2/m_\eta^2$. The dotted line represents the phase space distribution. The dashed line corresponds to the calculation at $O(p^6)$ without reduction of the resonances. The dash-dotted lines display the uncertainty in the reduction of meson resonances for different values of the parameter $Z_A^2$. The solid line corresponds to the values of the coefficients $L_i$ and $d_i$ used in Ref. [11].

$\gamma\gamma \to \pi^0\pi^0$ cross section results from the interference between the Born amplitude on the one hand and one- and two-loop amplitudes on the other hand. Thus the experimental data are not sensitive enough to the various Born contributions described by $d_i$. On the other hand, the Born contribution is dominating in the $\eta \to \pi^0\gamma\gamma$ decay. In Fig. 2 we show the normalized differential decay probability as a function of $m^2_{\gamma\gamma}/m^2_\eta$. In this case the differential distribution is very sensitive to the input parameters $d_i$. Thus data of the differential distribution would be of great value for constraining these parameters.

In conclusion, a self-consistent, quantitative description of $\gamma\gamma \to \pi^0\pi^0$ *and* $\eta \to \pi^0\gamma\gamma$ data at $O(p^6)$ is still problematic. A good description of the $\gamma\gamma \to \pi^0\pi^0$ cross section has been achieved whereas a satisfactory, quantitative prediction of the decay width seems to be beyond the reach of an ordinary calculation at $O(p^6)$.

The authors gratefully acknowledge fruitful discussions with C. Bruno, G. Ecker, J. Gasser, E. A. Kuraev, H. Leutwyler, M. R. Pennington, V. N. Pervushin, A. Schaale and M. K. Volkov. One of the authors (A. A. Bel'kov) would like to thank SFB 201 of the Deutsche Forschungsgemeinschaft for its hospitality and financial support during his stay at Mainz. This work was supported by the Russian Foundation for Fundamental Research under grant No. 94-02-03973.

# References

[1] M. V. Terent'ev, Sov. J. Nucl. Phys. **16** (1973) 87.

[2] M. K. Volkov and V. N. Pervushin, Sov. J. Nucl. Phys. **22** (1976) 179.

[3] B. R. Holstein, Comments Nucl. Part. Phys. **19** (1990) 221;
D. Drechsel, L. V. Fil'kov, Z. Phys. **A349** (1994) 177.

[4] A. A. Bel'kov and V. N. Pervushin, Sov. J. Nucl. Phys. **40** (1984) 616;
A. A. Bel'kov, E. A. Kuraev, and V. N. Pervushin, Sov. J. Nucl. Phys. **40** (1984) 942.

[5] Crystal Ball Collaboration (H. Marsiske et al.), Phys. Rev. **D41** (1990) 3324.

[6] S. Weinberg, Physica **96A** (1979) 327.

[7] J. Gasser and H. Leutwyler, Ann. Phys. **158** (1984) 142; Nucl. Phys. **B250** (1985) 465.

[8] J. Bijnens and F. Cornet, Nucl. Phys. **B296** (1988) 557;
J. F. Donoghue, B. R. Holstein, and Y. C. Lin, Phys. Rev. **D37** (1988) 2423.

[9] J. Bijnens, S. Dawson, and G. Valencia, Phys. Rev. **D44** (1991) 3555.

[10] J. F. Donoghue and B. R. Holstein, Phys. Rev. **D48** (1993) 137;
D. Morgan and M. R. Pennington, Phys. Lett. **B272** (1991) 134;
M. R. Pennington, in *The DAΦNE Physics Handbook*, Vol. II, p. 379 (Ed. L. Maiani, C. Pancheri and N. Paver), INFN, Frascati, 1992.

[11] S. Bellucci, J. Gasser and M. E. Sainio, Nucl. Phys. **B423** (1994) 80; ibid **B431** (1994) 413 (Erratum).

[12] M. Knecht, B. Moussallam and J. Stern, Nucl. Phys. **B429** (1994) 125.

[13] Ll. Ametller, J. Bijnens, A. Bramon and F. Cornet, Phys. Lett. **B276** (1992) 185.

[14] Particle Data Group, L. Montanet et al., Review of Particle Properties, Phys. Rev. **D50** (1994) 1173.

[15] S. Bellucci and C. Bruno, Report BUTP-94/26 (1994), hep-ph/9502243.

[16] P. Ko, Phys. Lett. **B349** (1995) 555.

[17] J. Bijnens, C. Bruno and E. de Rafael, Nucl. Phys. **B390** (1993) 501.

[18] J. N. Ng and D. J. Peters, Phys. Rev. **D47** (1993) 4939.

[19] M. K. Volkov, Ann. Phys. **157** (1984) 282; Sov. J. Part. Nucl. **17** (1986) 186; ibid. **24** (1993) 35;
D. Ebert and H. Reinhardt, Nucl. Phys. **B271** (1986) 188;
S. P. Klevansky, Rev. Mod. Phys. **64** (1992) 649;
A. A. Bel'kov et al., Int. J. Mod. Phys. **C4** (1993) 775; Int. J. Mod. Phys. **A8** (1993) 1313.

[20] Y. Nambu and G. Jona-Lasinio, Phys. Rev. **122** (1961) 345; ibid. **124** (1961) 246.

[21] H. W. Fearing and S. Scherer, TRIUMF report TRI-PP-94-68 (1994), hep-ph/9408346.

[22] M. K. Volkov, Ann. Phys. **49** (1968) 202; Fortschr. Phys. **22** (1974) 499.

[23] J. Schwinger, Phys. Rev. **82** (1951) 664;
B. S. De Witt, *Dynamical theory of groups and fields*, Gordon and Breach, New York (1965);
R. D. Ball, Phys. Rep. **182** (1989) 1.

[24] A. A. Bel'kov, A. V. Lanyov and A. Schaale, Dubna report JINR E2-95-238 (1995), hep-ph/9506237, to appear in *Proc. IV Int. Workshop on Software Engineering, Artificial Intelligence for High Energy and Nuclear Physics*, Pisa (Italy), Apr. 3–8, 1995, Ed. B. Denby.

[25] A. A. Bel'kov, A. V. Lanyov, A. Schaale and S. Scherer, Acta Physica Slovaca **45** (1995) 121.

[26] G. Ecker, J. Gasser, A. Pich and E. de Rafael, Nucl. Phys. **B321** (1989) 311;
J. F. Donoghue, C. Ramirez, and G. Valencia, Phys. Rev. **D39** (1989) 1947.

[27] A. A. Bel'kov, A. V. Lanyov and A. Schaale, Acta Physica Slovaca **45** (1995) 135.

[28] H. Reinhardt and B. V. Dang, Nucl. Phys. **A500** (1989) 563.

Received by Publishing Department
on June 23, 1995.

Бельков А.А., Ланев А.В., Шерер Ш. E2-95-266

Процессы $\gamma\gamma \to \pi^0\pi^0$ и $\eta \to \pi^0\gamma\gamma$ в $p^6$-порядке в модели НИЛ

Обсуждаются процессы $\gamma\gamma \to \pi^0\pi^0$ и $\eta \to \pi^0\gamma\gamma$ в $p^6$-порядке импульсного разложения. Вычисления включают древесные, одно- и двухпетлевые диаграммы кирального эффективного лагранжиана, полученного из бозонизации модели НИЛ. Показана важность учета интегрирования (редукции) мезонных резонансов. Окончательные результаты по сечению $\gamma\gamma \to \pi^0\pi^0$ находятся в хорошем согласии с экспериментальными данными коллаборации Crystal Ball. Для ширины распада $\eta \to \pi^0\gamma\gamma$ получена оценка 0,11 эВ, в то время как эксперимент дает (0,84 ± 0,18) эВ. Использование эмпирических параметров модели векторной доминантности приводит к величине 0,35 эВ. Получены предсказания для дифференциальной вероятности распада как функции $m^2_{\gamma\gamma}/m^2_\eta$.

Работа выполнена в Лаборатории сверхвысоких энергий ОИЯИ.

Препринт Объединенного института ядерных исследований. Дубна, 1995

Bel'kov A.A., Lanyov A.V., Scherer S. E2-95-266

Processes $\gamma\gamma \to \pi^0\pi^0$ and $\eta \to \pi^0\gamma\gamma$ at $O(p^6)$ in the NJL Model

We discuss the processes $\gamma\gamma \to \pi^0\pi^0$ and $\eta \to \pi^0\gamma\gamma$ at $O(p^6)$ in the momentum expansion. The calculation involves tree-level, one-loop and two-loop diagrams of a chiral effective lagrangian which is obtained by a bosonization of the NJL model. The importance of integrating out meson resonances (reduction) is pointed out. Our final results for the total cross section of $\gamma\gamma \to \pi^0\pi^0$ are in good agreement with the experimental data of the Crystal Ball Collaboration. For the width of the $\eta \to \pi^0\gamma\gamma$ decay we obtain the value 0.11 eV which has to be compared with the experimental value of (0.84 ± 0.18) eV. Alternatively, taking empirical parameters from a vector-meson-dominance model the prediction for the decay width is 0.35 eV. We present a prediction for the differential decay probability as a function of $m^2_{\gamma\gamma}/m^2_\eta$.

The investigation has been performed at the Laboratory of Particle Physics, JINR.

Preprint of the Joint Institute for Nuclear Research. Dubna, 1995

Макет Т.Е.Попеко

Подписано в печать 1.08.95
Формат 60×90/16. Офсетная печать. Уч.-изд.листов 1,38
Тираж 460. Заказ 48457. Цена 828 р.

Издательский отдел Объединенного института ядерных исследований
Дубна Московской области